

Speculative Decoding Reimagined for Multimodal Large Language Models

Luxi Lin^{1*}, Zhihang Lin^{1,2*}, Zhanpeng Zeng¹, Rongrong Ji^{1†}

¹Key Laboratory of Multimedia Trusted Perception and Efficient Computing,
Ministry of Education of China, Xiamen University, 361005, P.R. China

²Shanghai Innovation Institute

lewuloo@gmail.com, lzhedu@foxmail.com, wispcpen@gmail.com, rrji@xmu.edu.cn

*Equal contribution †Corresponding author

Abstract

This paper introduces Multimodal Speculative Decoding (MSD) to accelerate Multimodal Large Language Models (MLLMs) inference. Speculative decoding has been shown to accelerate Large Language Models (LLMs) without sacrificing accuracy. However, current speculative decoding methods for MLLMs fail to achieve the same speedup as they do for LLMs. To address this, we reimagine speculative decoding specifically for MLLMs. Our analysis of MLLM characteristics reveals two key design principles for MSD: (1) Text and visual tokens have fundamentally different characteristics and need to be processed separately during drafting. (2) Both language modeling ability and visual perception capability are crucial for the draft model. For the first principle, MSD decouples text and visual tokens in the draft model, allowing each to be handled based on its own characteristics. For the second principle, MSD uses a two-stage training strategy: In stage one, the draft model is trained on text-only instruction-tuning datasets to improve its language modeling ability. In stage two, MSD gradually introduces multimodal data to enhance the visual perception capability of the draft model. Experiments show that MSD boosts inference speed by up to $2.29\times$ for LLaVA-1.5-7B and up to $2.46\times$ for LLaVA-1.5-13B on multimodal benchmarks, demonstrating its effectiveness. Our code is available at <https://github.com/Lyn-Lucy/MSD>.

1. Introduction

Multimodal large language models (MLLMs) [4, 24, 31, 32] have made significant strides in cross-modal applications such as visual question answering (VQA) [19], visual captioning [11, 37], and multimodal chatbots [1, 41]. MLLMs usually consist of a vision encoder, a projection layer, and a large language model (LLM). Through vi-

Table 1. Average acceptance length of draft models with different predictive objectives on three multimodal tasks: ChartQA [35], TextVQA [40], and Hallusion [20], using LLaVA-1.5-7B [31] as the target model.

Type	ChartQA	TextVQA	Hallusion	Average
Token-level	1.69	1.98	1.77	1.81
Feature-level	3.25	3.63	3.54	3.47

sual instruction tuning, MLLMs achieve remarkable performance in multimodal tasks [31]. However, MLLMs inherit the large parameter size of LLMs, leading to substantial computational overhead and slow inference speed. These limitations have become critical bottlenecks for real-world applications where low latency and high throughput are essential for practical deployment.

To optimize the inference efficiency of MLLMs, researchers have proposed various methods, such as pruning [9, 44], quantization [25, 42], distillation [43], and efficient architecture design [29, 36]. Although these methods improve the inference efficiency of MLLMs, they often compromise their accuracy. Such trade-offs between efficiency and accuracy are undesirable in real-world applications, where high-quality and reliable responses are indispensable. Thus, accelerating MLLM inference without sacrificing accuracy remains a critical challenge.

Speculative decoding (SD) has been proven to be an effective lossless inference acceleration method in LLMs [23]. SD uses a lightweight draft model to generate multiple candidate tokens, which are then verified in parallel by a target model (LLM). SD breaks the paradigm of generating one token at a time and can significantly speed up the inference of LLMs. As the main computational overhead of MLLMs comes from the LLM portion, SD can also be extended to MLLMs. Recently, Gagrani *et al.* [18] conduct an initial exploration of speculative decoding in MLLMs, showing that draft models which are trained on text-only datasets can accelerate the inference of MLLMs.

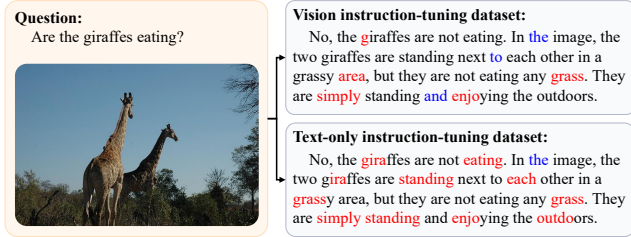


Figure 1. Comparison of models trained on text-only and vision instruction data, using LLaVA-1.5-7B as the target model. Black tokens are judged correct; red and blue tokens mark visual-related and unrelated errors, respectively.

However, the average acceptance length of their draft model is only 2.5, which is far from the average acceptance length (5) of the state-of-the-art draft model in LLMs [18,27]. This discrepancy highlights that the existing speculative decoding methods for MLLMs have not fully utilized the potential of speculative decoding. Designing an effective speculative decoding method to accelerate MLLM inference remains an open and pressing challenge.

Based on the predictive objective of draft models, speculative decoding methods can be divided into two categories: token-level and feature-level. Token-level methods like MEDUSA [5] and Lookahead [17] directly predict the next token, while feature-level methods like Eagle [28] predict the feature of the next token. Feature-level methods achieve a higher acceleration ratio and average acceptance length than token-level methods in LLMs [28]. To validate whether this conclusion still holds in MLLMs, we conduct an ablation study comparing the average acceptance length of token-level and feature-level SD methods in MLLMs. As shown in Table 1, the feature-level SD consistently outperforms the token-level SD in MLLMs. However, the average acceptance length of feature-level SD in MLLMs still lags behind that of LLMs, indicating that existing SD methods cannot be directly applied to MLLMs. Thus, we need to reimagine the design of SD for MLLMs to fully leverage its acceleration potential.

As ablation studies show that the feature-level SD outperforms the token-level SD in MLLMs, we take the feature-level speculative decoding method as our baseline and redesign it based on MLLMs’ characteristics. The first discrepancy between MLLMs and LLMs is that the draft model in MLLMs not only processes text tokens but also visual tokens. A critical question arises: should tokens from different modalities be handled differently? To answer this question, we analyze the characteristics of text and visual tokens. Text tokens are derived from a sequence of words processed through a tokenizer and are only related to the previous tokens in the sequence. In contrast, visual tokens are obtained by processing images with vision encoders like CLIP [38], then unfolded into one-dimensional

sequences, and finally projected into the word embedding space through a projection layer. Visual tokens are related to all other visual tokens in the sequence, which show a great difference from text tokens. These distinct characteristics imply that visual and text tokens should not be processed indiscriminately in the draft model.

The second key difference between MLLMs and LLMs is their training datasets. LLMs, trained on text-only data, excel in language modeling, predicting the next token based on rich textual context. MLLMs, however, are trained on multimodal data, possessing both language modeling and visual perception abilities. The draft model of LLMs is typically trained on text-only instruction-tuning datasets. [2] A natural question is whether MLLMs’ draft model should also be trained on vision instruction-tuning datasets. To answer this question, we respectively train the draft model on a text-only and vision instruction-tuning dataset. As shown in Figure 1, the draft model trained on a text-only instruction-tuning dataset fails to generate the candidate tokens that need visual perception, such as “eating” and “giraffe”. While the draft model trained on a vision instruction-tuning dataset struggles with non-visual linguistic elements, such as common function words like “the” and “to”. This suggests that both language modeling and visual perception are critical for the draft model in MLLMs, and the draft model should be trained on both text-only and vision instruction-tuning datasets.

In this paper, we propose Multimodal Speculative Decoding (MSD), a novel speculative decoding method tailored for MLLMs. Our in-depth analysis of MLLMs’ characteristics leads to two key design principles for MSD. 1) The draft model should decouple the processing of text and visual tokens, allowing them to be processed in a manner that aligns with their unique characteristics. 2) The draft model should be trained on both text-only and vision instruction-tuning datasets, ensuring that it possesses strong language modeling and visual perception capabilities. For the first principle, MSD concatenates the features of text tokens with next-token embeddings, while directly inputting the features of visual tokens into the draft model. For the second principle, MSD employs a two-stage training strategy for the draft model. In the first stage, MSD focuses on strengthening the draft model’s language modeling ability by training it on text-only instruction-tuning datasets. In the second stage, MSD gradually introduces multimodal data to enhance the draft model’s visual perception capability.

We evaluate MSD on various multimodal tasks, including visual question answering [19, 21], document understanding [35, 40], and comprehensive benchmarking tasks [16, 33]. Experiments show that MSD boosts inference speed by up to $2.29\times$ for LLaVA-1.5-7B and up to $2.46\times$ for LLaVA-1.5-13B on multimodal benchmarks, demonstrating its effectiveness.

2. Related work

2.1. Efficient inference for MLLMs

Researchers are actively exploring ways to improve the inference efficiency of Multimodal Large Language Models (MLLMs) as their applications continue to expand. These methods fall into two categories: lossy acceleration and lossless acceleration. Lossy acceleration includes techniques like pruning [43], quantization [25, 42], efficient network design [29, 36], and token reduction [6, 9, 39, 44]. These methods improve efficiency by simplifying the model or reducing modules, tokens, or parameters, balancing speed and performance. For example, TinyLLaVA [50] and LLaVA-Phi [51] replace large backbones with compact alternatives. TokenPacker [26] condenses features to reduce the number of tokens, while FastV [8] and VTW [30] discard unimportant visual tokens in the deep layers of MLLMs. Lossless acceleration optimizes computation without sacrificing accuracy, using techniques like FlashAttention [14, 15] and PageAttention [22] to reduce memory and computation costs.

2.2. Speculative decoding

Speculative decoding [23] utilizes a draft model to generate multiple candidate tokens, which are then validated by a target model, significantly speeding up LLM decoding. For example, Medusa [5] uses multiple prediction heads to generate several tokens at once. Eagle [27, 28] and HASS [48] employ a lightweight single-layer Transformer to predict the hidden state of the next token. SPACE [46] enables parallel token generation and validation through semi-autoregressive fine-tuning and automatic correction decoding algorithms. Self-speculative decoding [47] skips intermediate layers selectively, using its own model to generate draft tokens. However, speculative decoding remains largely unexplored in MLLMs.

Recently, Gagrani *et al.* [18] apply speculative decoding to MLLMs, showing that draft models trained on text-only datasets outperform those using multimodal datasets. However, their average acceptance length still lags behind that of LLMs. Our experiments demonstrate that visual information is essential for enhancing draft quality, underscoring the need to reimagine speculative decoding in MLLMs to fully realize its acceleration potential.

3. Background

3.1. Multimodal Large Language Model

There are various MLLMs architectures, such as LLaVA [31], Qwen-VL [3], InternVL [12], and mPLUG-Owl [45]. For clarity, we adopt the widely used LLaVA to illustrate the inputs of MLLMs.

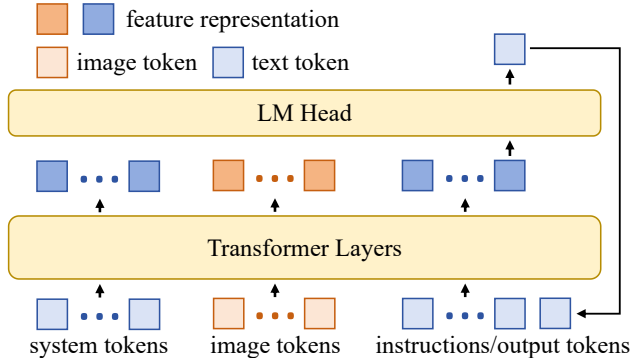


Figure 2. Input illustration of MLLMs. The input to MLLMs comprises two distinct token types: text and image tokens.

As shown in Figure 2, the input tokens of LLaVA consist of two distinct types: text tokens $\{t_0, t_1, \dots, t_n\}$ and image tokens $\{v_0, v_1, \dots, v_m\}$. The text tokens usually include system tokens, instruction tokens, and the output tokens generated by MLLMs. The text tokens are encoded into embeddings through the embedding layer $E_t(\cdot)$ of the LLM as:

$$e_{t_i} = E_t(t_i), \quad i \in [0, n]. \quad (1)$$

The image tokens are derived from the image, which go through a vision encoder $E_v(\cdot)$, e.g., CLIP, to extract visual features and then projected into the word embedding space of the LLM through a projection layer ($f_{mlp}(\cdot)$) as:

$$e_{v_i} = f_{mlp}(E_v(v_i)), \quad i \in [0, m]. \quad (2)$$

Finally, text tokens embeddings and image tokens embeddings are interweaved to form a multimodal input sequence:

$$e_{x_i} = [e_{t_0}, \dots, e_{t_p}, e_{v_0}, \dots, e_{v_m}, e_{t_{p+1}}, \dots, e_{t_n}], \quad i \in [0, m+n] \quad (3)$$

where p is the number of system tokens, n is the number of text tokens, and m is the number of image tokens. The multimodal embeddings e_{x_i} are then fed into the MLLM to generate the corresponding feature representations h_{x_i} , which are then processed by the MLLM's projection head to produce the final output token probabilities $p(x_{i+1}|x_{<i+1})$. The next output token x_{i+1} is generated by sampling from the output distribution $p(x_{i+1}|x_{<i+1})$ and is appended to the input sequence for the next decoding step.

LLaVA uses a two-stage training process. First, it freezes the vision encoder and LLM, and trains the projection layer $f_{mlp}(\cdot)$ on a large-scale image-text dataset to align visual tokens with the word embedding space of LLM. Then, it unfreezes the LLM and fine-tunes both the LLM and projection layer on a multimodal instruction-following dataset to produce the final MLLM.

3.2. Feature-level Speculative Decoding

Li *et al.* [28] propose feature-level speculative decoding to accelerate the autoregressive decoding of LLMs. The feature-level speculative decoding is a two-phase process that leverages a lightweight draft model to generate candidate token sequences, which are subsequently validated by the target model.

Feature-level Draft Phase The feature-level draft model M_q predicts the next token’s feature $h_{x_{i+1}}$ based on prefix hidden states $\{h_{x_0}, \dots, h_{x_i}\}$ and input token embeddings $\{e_{x_1}, \dots, e_{x_{i+1}}\}$ as:

$$\begin{aligned} h_{x_{i+1}} &= M_q(f_{x_0}, \dots, f_{x_i}); \\ f_{x_i} &= f_{\text{down}}(\text{Concat}(h_{x_i}, e_{x_{i+1}})). \end{aligned} \quad (4)$$

Here, $\text{Concat}(\cdot)$ concatenates features in the last dimension, and $f_{\text{down}}(\cdot)$ down-samples the concatenated feature to match the dimension of h_{x_i} . f_{x_i} is fed into a transformer layer that constitutes the draft model M_q . Then the predicted feature $h_{x_{i+1}}$ is passed through the target model’s projection head to obtain the predicted token probability $q(\hat{x}_{i+1}|x_{<i+1})$ as:

$$q(\hat{x}_{i+1}|x_{<i+1}) = f_{LM_{\text{head}}}(h_{x_{i+1}}). \quad (5)$$

This process is repeated for γ steps, generating a sequence of γ candidate tokens $\hat{x}_{i+1:i+\gamma}$ and their associated probabilities $q(\hat{x}_{i+n}|x_{<t+n})$ for $n = 1, \dots, \gamma$. A tree-structured attention mechanism [28] is employed in this phase. It constructs a hierarchical draft tree with depth m , generating more than m tokens through m forward passes. At each step, the model expands each leaf node by generating multiple candidate tokens in parallel, iteratively growing the tree breadth-wise.

Verification Phase The target model M_p verifies the candidate tokens in parallel by computing their probabilities $p(\hat{x}_{t+n}|x_{<t+n})$. The acceptance probability for a candidate token \hat{x}_{t+n} is defined as:

$$p_{\text{accept}}(\hat{x}_{t+n}) = \min \left(1, \frac{p(\hat{x}_{t+n}|x_{<t+n})}{q(\hat{x}_{t+n}|x_{<t+n})} \right). \quad (6)$$

If a token \hat{x}_{t+j} is rejected, subsequent tokens in the draft are discarded, and a new token is sampled from the adjusted distribution:

$$\begin{aligned} p_{\text{adjusted}} &= \text{norm} \left(\max \left(0, p(\hat{x}_{t+j}|x_{<t+j}) \right. \right. \\ &\quad \left. \left. - q(\hat{x}_{t+j}|x_{<t+j}) \right) \right) \end{aligned} \quad (7)$$

Here, the function $\text{norm}(\cdot)$ normalizes the adjusted distribution to ensure that it sums to one. If all candidate tokens are accepted, an additional token $\hat{x}_{t+\gamma+1}$ is sampled from the target model’s prediction distribution $p(\hat{x}_{t+\gamma+1}|x_{<t+\gamma+1})$.

3.3. Baseline Setting

In LLMs, feature-level speculative decoding attains a notably greater average acceptance length compared to token-level speculative decoding [28]. To validate whether this advantage holds in MLLMs, we conduct an ablation study on the LLaVA-1.5-7B model. The results in Table 1 show that feature-level speculative decoding still achieves significantly higher average acceptance length than token-level speculative decoding in MLLMs. However, the average acceptance length of state-of-the-art feature-level speculative decoding in LLMs has achieved 5, while the average acceptance length of feature-level speculative decoding in MLLMs is only 3.47. This indicates that the feature-level speculative decoding specifically designed for LLMs fails to fully exploit their acceleration advantages in MLLMs. Thus, we build on feature-level speculative decoding to reimagine speculative decoding in MLLMs.

4. Multimodal Speculative Decoding

In this section, we introduce Multimodal Speculative Decoding (MSD), a novel speculative decoding framework for MLLMs, as illustrated in Figure 3. The core design of MSD is motivated by two key discrepancies between LLMs and MLLMs: (1) The different input characteristics between LLMs and MLLMs. (2) The different training datasets between LLMs and MLLMs.

4.1. Decoupling Tokens of Different Modalities

The most obvious difference between LLMs and MLLMs lies in the number of modalities. The LLMs’ input consists solely of text modality, while MLLMs’ input not only includes text modality but also other modalities, such as visual modality in the case of LLaVA. A critical question arises: should input from different modalities be processed in the same way during drafting? To answer this question, we need to analyze the inherent characteristics of the input from different modalities.

In text modality, the input is a sequence of words, which are tokenized and embedded into a sequence of text tokens. In LLMs, each token’s prediction is only dependent on the previous tokens due to the causal self-attention mechanism, showing a clear sequential dependency. In contrast, in the visual modality, the input is images, which are divided into patches and then unfolded into a one-dimensional sequence of visual tokens. These visual tokens are encoded by a visual encoder, *e.g.*, CLIP, which uses bidirectional self-attention to process the image features. Visual tokens are related to all visual tokens in the image, rather than just the previous tokens. In traditional feature-level speculative decoding of LLMs [28], the hidden state of the current token is concatenated with the embedding of the next token to reduce the ambiguity of autoregressive generation, as formu-

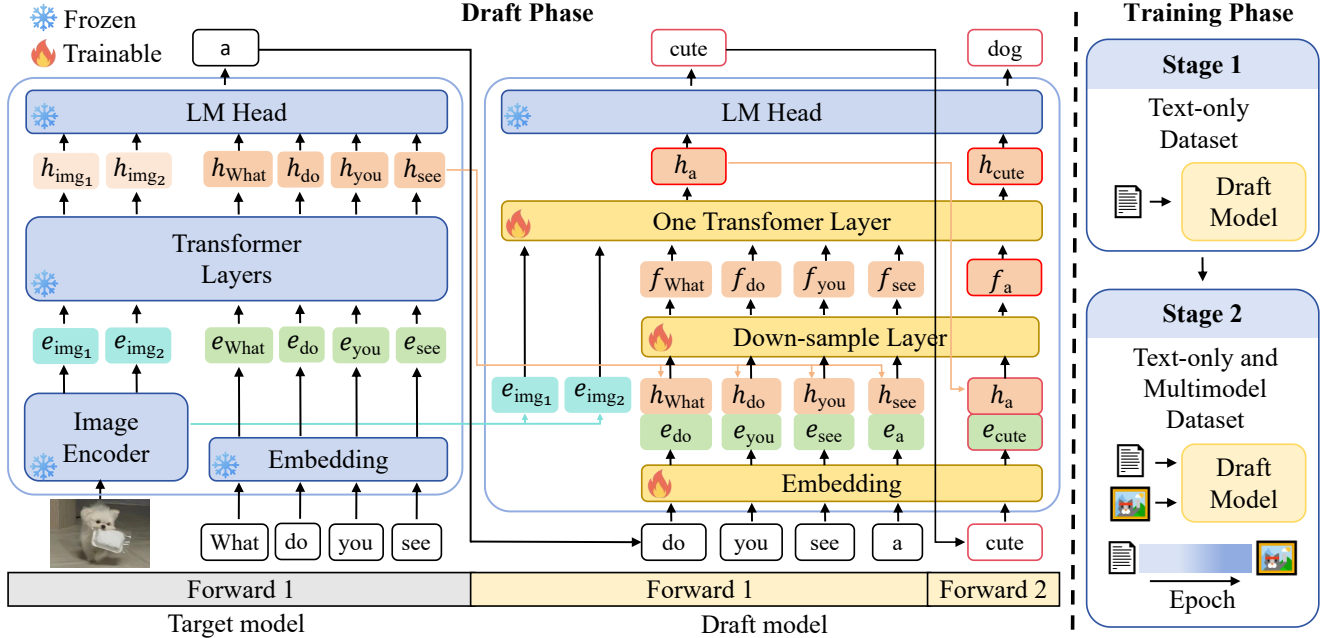


Figure 3. The framework of Multimodal Speculative Decoding (MSD). The left illustrates the draft phase, while the right illustrates the training phase. e represents token embeddings, and f denotes the concatenated features. Red-bordered tokens are predicted by the draft model. MSD concatenates text token hidden states with the next token embeddings, while directly inputting visual tokens embedding without concatenation during drafting. MSD trains the draft model using a text-only instruction-tuning dataset in Stage 1, and then gradually introduces a multimodal instruction-tuning dataset in Stage 2.

lated in Eq. (4). This design is valid for text tokens, as they have a clear sequential dependency. However, for visual tokens, the displacement concatenation operation may hurt the information encoded in the visual tokens, as they do not have sequential dependency like text tokens. Thus, visual tokens should be processed differently from text tokens.

Based on the analysis of the inherent characteristics of different modal inputs, we decouple the processing of text and visual tokens in the draft model of MSD, as illustrated in Figure 3. Specifically, for text tokens, we keep the displacement concatenation operation in Eq. (4), while for visual tokens, we directly use the visual token embeddings in Eq. (2) as inputs to the draft model. The draft model predicts the next token’s feature based on the concatenated text token features and the visual token embeddings as:

$$h_{x_{i+1}} = M_q(f_{x_0}, \dots, f_{x_i}), \quad (8)$$

where

$$f_{x_i} = \begin{cases} f_{down}(\text{Concat}(h_{x_i}, e_{x_{i+1}})), & \text{if } x_i \text{ is text token,} \\ e_{x_i}, & \text{if } x_i \text{ is visual token.} \end{cases} \quad (9)$$

Here $\text{Concat}(\cdot)$ is the concatenation operation and h_{x_i} is the feature of e_{x_i} in the target model. The remaining progress is similar to the original feature-level speculative decoding detailed in Sec. 3.2.

As shown in Sec. 5.3, by decoupling the processing of text and visual tokens, MSD achieves a significant performance improvement over the baseline. This performance gain supports our analysis of the inherent characteristics of different modal inputs, highlighting the necessity of incorporating these characteristics into the design of the draft model for MLLMs.

4.2. Two-Stage Training for Draft Models

The second key difference between LLMs and MLLMs lies in the training datasets. LLMs are typically trained on large-scale text-only datasets, while MLLMs are trained on vision instruction-tuning datasets. Different training datasets lead to different model capabilities. LLMs achieve strong language modeling capability by training on text-only datasets. MLLMs, on the other hand, acquire both language modeling and visual perception capabilities through fine-tuning a well-trained LLM on vision instruction-tuning datasets. For the draft model in LLMs, it is natural to be trained on text-only datasets, as there is no other modality involved. The draft model in LLMs is typically fine-tuned on text-only instruction-tuning datasets. However, for the draft model in MLLMs, we need to answer the questions: which dataset should we use to train the draft model of MLLMs? Is the visual instruction-tuning dataset enough for training the draft model?

Table 2. Average acceptance length (τ) of the draft model trained on different datasets across three multimodal tasks: ChartQA [35], TextVQA [40], and Hallusion [20]. The evaluation uses LLaVA-1.5-7B [31] as the target model.

Method	ChartQA	TextVQA	Hallusion	Average
Text-only instruction-tuning dataset	2.59	3.05	2.95	2.86
Vision instruction-tuning dataset	3.25	3.63	3.54	3.47

To address this, we conduct an ablation study on the training datasets used for the draft model. Specifically, we respectively train the draft model on a text-only instruction-tuning dataset and a vision instruction-tuning dataset and then evaluate their performance on multimodal benchmarks. As shown in Table 2, the draft model trained on the text-only instruction-tuning dataset achieves an average acceptance length of 2.86, while the draft model trained on the vision instruction-tuning dataset achieves an average acceptance length of 3.47. Though the draft model trained on the vision instruction-tuning dataset performs better than that trained on the text-only dataset, it still falls short of the average acceptance length of speculative decoding in LLMs.

To dive deeper into the reasons behind this performance gap, we visualize the tokens rejected by the target model in Figure 1. We find that the draft model trained on the vision instruction-tuning dataset tends to generate incorrect tokens that are unrelated to visual content, such as prepositions and conjunctions, such as “to” and “and”. While the draft model trained on the text-only instruction-tuning dataset is capable of generating these tokens, it fails to generate tokens that require visual perception, such as “eating” and “giraffe”. This indicates that the draft model trained on the vision instruction-tuning dataset is poor at language modeling, while the draft model trained on the text-only dataset is poor at visual perception. Thus, it is not enough to train the draft model of MLLMs solely on the vision instruction-tuning dataset. The draft model should be trained on both text-only instruction-tuning datasets and vision instruction-tuning datasets, as language modeling ability and visual perception ability are both important for the draft model. Based on the analysis above, we propose a two-stage training strategy for the draft model of MLLMs, which consists of two stages: (1) fundamental language modeling training and (2) progressive multimodal data mix training.

Stage 1: Fundamental Language Modeling Training

In the first stage, the draft model is trained on a text-only instruction-tuning dataset D_{text} from LLaMA. [2] This stage aims to solidly build the draft model’s foundational language modeling abilities, minimizing the likelihood of producing wrong tokens unrelated to visual content during the drafting stage.

Stage 2: Progressive Multimodal Data Mix Training

In the second stage, we introduce a progressive multimodal data mix training strategy to enhance the draft model’s visual perception capability. Specifically, we train the draft model on a mix of a text-only instruction-tuning dataset D_{text} and a visual instruction-tuning dataset D_{visual} as follows:

$$D_{mix}^t = D_{text} \cdot \frac{T-t}{T} + D_{visual} \cdot \frac{t}{T}, \quad (10)$$

where T is the total number of training epochs and D_{mix}^t is the mixed training dataset at epoch t . The progressive multimodal data mix training strategy allows the draft model to gradually acquire visual perception capability while effectively retaining its language modeling capability, as discussed in Sec. 5.3.

5. Experiments

5.1. Experimental Setting

5.1.1 Training Details.

We assess the performance of MSD on widely used MLLMs, such as LLaVA-1.5-7B [31] and LLaVA-1.5-13B. The training dataset sizes for both text-only and visual instruction-tuning datasets are identical. Specifically, the text-only instruction-tuning dataset consists of 68,000 randomly selected dialogue samples from ShareGPT [2], while the visual instruction-tuning dataset includes 68,000 randomly selected samples from LLaVA-Instruct-150K [31]. We train draft models on four NVIDIA 4090 GPUs for 20 epochs, with a batch size of 4 and a learning rate of 5e-5. We use cosine learning rate scheduling for training.

5.1.2 Benchmarks

We evaluate MSD on various multimodal benchmarks. The chosen benchmarks include visual question answering such as VQA_{v2} [19] and AI2D [21], document and chart understanding tasks including ChartQA [35] and TextVQA [40], multimodal hallucination evaluation benchmarks such as Hallusion [20], and comprehensive benchmarks like MMB_{EN} [33] and MME [16]. Following prior work [28], we conduct our evaluation on the randomly sampled subset of benchmarks, as speculative decoding is a lossless acceleration technique. The number of evaluation samples is set to 100 for each benchmark.

5.1.3 Metrics

We assess the performance of our MSD using the following widely used metrics in speculative decoding [28]:

Table 3. Speedup ratios SR and average acceptance lengths τ of different methods on VQAv2 [19], AI2D [21], SQA_Image [34], ChartQA [35], TextVQA [40], Hallusion [20], MMB_EN [33], and MME [16] benchmarks with temperature $T \in \{0, 1\}$. **Bold** denotes the best results.

Model	Method	VQAv2		AI2D		SQA_Image		ChartQA		TextVQA		Hallusion		MMB_EN		MME	
		SR	τ														
Temperature = 0																	
LLaVA-1.5-7B	Baseline	2.09x	4.55	1.75x	3.34	1.72x	3.41	1.73x	3.25	1.75x	3.63	1.85x	3.54	1.73x	3.59	1.84x	3.53
	Lookahead [17]	1.28x	1.33	1.37x	1.45	1.35x	1.45	1.32x	1.42	1.22x	1.31	1.41x	1.50	1.32x	1.41	1.34x	1.40
	Text_Only [18]	1.79x	3.63	1.57x	2.93	1.61x	3.12	1.42x	2.59	1.55x	3.05	1.59x	2.95	1.60x	3.20	1.68x	3.14
	MSD	2.19x	4.95	2.09x	4.21	2.03x	4.33	2.13x	4.26	2.02x	4.3	2.29x	4.63	2.06x	4.62	2.15x	4.31
LLaVA-1.5-13B	Baseline	2.17x	4.27	2.02x	3.38	1.77x	3.16	1.87x	3.16	1.78x	3.33	2.02x	3.40	1.97x	3.39	2.02x	3.43
	Lookahead	1.21x	1.28	1.31x	1.40	1.32x	1.42	1.30x	1.40	1.24x	1.31	1.37x	1.46	1.35x	1.41	1.27x	1.32
	Text_Only	1.81x	3.30	1.89x	3.11	1.74x	3.03	1.74x	2.89	1.56x	2.80	1.78x	2.96	1.83x	3.07	1.76x	2.88
	MSD	2.21x	4.47	2.32x	4.08	2.13x	4.11	2.25x	4.00	2.02x	4.11	2.46x	4.37	2.34x	4.28	2.28x	4.04
Temperature = 1																	
LLaVA-1.5-7B	Baseline	1.64x	3.27	1.42x	2.62	1.44x	2.70	1.40x	2.57	1.41x	2.71	1.53x	2.83	1.47x	2.82	1.43x	2.67
	Lookahead	1.15x	1.24	1.22x	1.29	1.20x	1.30	1.19x	1.28	1.14x	1.21	1.30x	1.38	1.22x	1.29	1.16x	1.24
	Text_Only	1.48x	2.89	1.33x	2.45	1.39x	2.59	1.22x	2.21	1.29x	2.41	1.37x	2.50	1.43x	2.67	1.33x	2.46
	MSD	1.73x	3.57	1.62x	3.13	1.67x	3.29	1.66x	3.19	1.55x	3.12	1.81x	3.51	1.71x	3.51	1.60x	3.10
LLaVA-1.5-13B	Baseline	1.82x	3.18	1.62x	2.62	1.60x	2.67	1.61x	2.61	1.53x	2.57	1.72x	2.83	1.63x	2.75	1.63x	2.65
	Lookahead	1.13x	1.20	1.24x	1.29	1.20x	1.27	1.22x	1.29	1.13x	1.21	1.24x	1.33	1.21x	1.30	1.10x	1.20
	Text_Only	1.54x	2.57	1.54x	2.51	1.55x	2.55	1.49x	2.37	1.33x	2.19	1.58x	2.59	1.57x	2.57	1.46x	2.37
	MSD	1.91x	3.44	1.85x	3.07	1.86x	3.27	1.87x	3.12	1.78x	3.07	2.01x	3.40	1.96x	3.37	1.79x	2.98

Average Acceptance Length τ This metric measures the average number of tokens accepted by the target model in each drafting-verification cycle. It reflects the effectiveness of the draft model in predicting tokens that align with the target model’s output. A higher average acceptance length indicates better draft accuracy and fewer verification rounds required.

Acceptance Rate α The acceptance rate α represents the ratio of accepted to candidate tokens during drafting. In this metric, we use chain drafts, where the draft model generates one token per forward pass. Since the draft model predicts features autoregressively, errors may accumulate across steps. Following previous work [28], we measure the acceptance rate as $n\text{-}\alpha$, where $n\text{-}\alpha$ is the acceptance rate of the n -th predicted token during drafting.

Speedup Ratio SR The speedup ratio (SR) measures the relative acceleration of speculative decoding compared to vanilla autoregressive decoding. Given an average acceptance rate $\alpha \in [0, 1]$ and a speculative length γ , the expected number of accepted tokens per verification step is defined as [7]:

$$\omega(\gamma, \alpha) := \mathbb{E}(\#\text{generated tokens}) = \frac{1 - \alpha^{\gamma+1}}{1 - \alpha}. \quad (11)$$

Including profiling time $T_{profiling}$ and output length N , the speedup ratio is calculated as:

$$SR = \frac{\text{Time(Normal Decoding)}}{\text{Time(Speculative Decoding)}} = \frac{N \cdot T_p + T_{profiling}}{N \cdot \left(\frac{\gamma \cdot T_q + T_v(\gamma)}{\omega(\gamma, \alpha)} \right) + T_{profiling}}, \quad (12)$$

where T_p is the time the target model takes to generate one token, and T_q is the time for the draft model. $T_v(\gamma)$ denotes the verification time of the target model for γ tokens. It is important to note that the profiling time $T_{profiling}$, which depends on the input length, and the output length N , significantly impacts the speedup ratio.

5.2. Main Results

In our experiments, we compare MSD with the following methods: (1) **Baseline**: The feature-level speculative decoding method defined in Sec. 3.3, which concatenates the hidden states from the target model with the next token embeddings on the draft model. (2) **Lookahead**: A training-free speculative decoding method for LLMs [17]. Lookahead generates n -gram sequences using Jacobi iteration during drafting, which are then verified by the target model. We extend this method to LLaVA for comparison. (3) **Text_Only**: Based on the findings of Gagrani et al. [18], which show that text-only input can perform as well as models using visual features. This draft model uses only the text part of the input question, ignoring visual features completely. Table 3 shows our experimental results, including the average acceptance length and speedup ratio for each method across different tasks, temperatures, and model sizes.

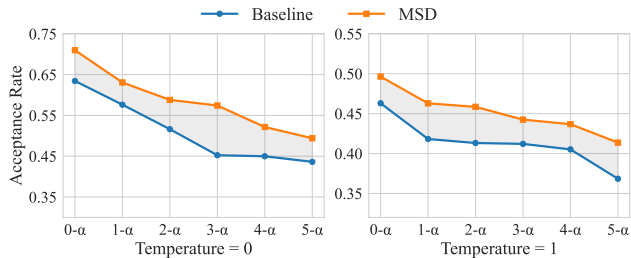


Figure 4. Comparison of acceptance rates between Baseline and MSD across different temperatures on a randomly sampled subset of 100 samples from TextVQA.

Comparison with Other Methods As shown in Table 3, our MSD clearly outperforms other methods across all tasks and model sizes, achieving the highest average acceptance lengths and speedup ratios. Notably, for LLaVA-1.5-7B [31] at Temperature = 0, MSD achieves an average acceptance length of 4.63 on the Hallusion [20] benchmark, surpassing the Baseline by 1.09 tokens and the previous state-of-the-art method Text_Only [18] by 1.68 tokens, resulting in a speedup ratio of 2.29 \times . Text_Only achieves an average acceptance length of just 2.59 on the ChartQA [35] benchmark, where visual information is critical for answering questions. This underscores the limitations of text-only input in multimodal tasks, as it overlooks crucial visual information. Both MSD and Baseline incorporate visual and textual features during drafting, leading to better average acceptance lengths and speedup ratios compared to Text_Only. MSD outperforms Baseline across all tasks and model sizes. The advantages of MSD stem from (1) a more effective way of handling visual tokens, ensuring both visual and textual inputs are properly processed during drafting, and (2) a two-stage training strategy that enables the draft model to acquire both strong language modeling and visual perception capabilities.

Impact of Temperature Settings Under the setting Temperature = 1, both the average acceptance length and speedup ratio decrease for all methods. This is expected, since higher temperatures and more relaxed sampling lead to more flattened probability distributions, which increases the possibility of predicting tokens with low probability during drafting. In this setting, MSD still maintains an average

Table 4. Ablation study on the contributions of MSD components, evaluated by average acceptance length.

Model	ChartQA \uparrow	AI2D \uparrow	MMB \uparrow	Hallusion \uparrow	Average
Baseline	3.25	3.34	3.59	3.54	3.43
+ Input Tokens Decoupling	3.80 (+0.55)	3.71 (+0.37)	4.06 (+0.47)	3.94 (+0.40)	3.88 (+0.45)
+ Two-Stage Training	4.05 (+0.80)	3.99 (+0.65)	4.32 (+0.73)	4.33 (+0.79)	4.17 (+0.74)
MSD	4.26 (+1.01)	4.21 (+0.87)	4.62 (+1.03)	4.63 (+1.09)	4.43 (+1.00)

Table 5. Ablation study on different strategies for handling visual tokens, evaluated by average acceptance length.

Method	ChartQA	AI2D	MMB	Hallusion
Baseline	3.25	3.34	3.59	3.54
Visual Feature	3.78 (+0.53)	3.66 (+0.32)	4.01 (+0.42)	3.94 (+0.40)
Visual embedding	3.80 (+0.55)	3.71 (+0.37)	4.06 (+0.47)	3.94 (+0.40)

acceptance length above 3 across all tasks, outperforming other methods, further demonstrating its robustness.

Comparing Speedup Ratio Between MLLM and LLM

MSD narrows the gap between the average acceptance length of MLLMs and LLMs. However, its speedup ratio is still lower than that of speculative decoding in LLMs. This difference mainly comes from the varying input and output lengths in MLLM and LLM benchmarks. We statistic the average input and output lengths of the benchmarks used in MLLMs and LLMs. For LLM benchmarks like MT-Bench [49], HumanEval [10], and GSM8K [13], the average input and output lengths of LLM’s are 428 and 388, respectively. In contrast, the average input and output lengths of MLLM’s benchmarks such as ChartQA [35], TextVQA [40], VQAv2 [19], and Hallusion [20] are 624 and 85. The longer input length in MLLM benchmarks increases the $T_{profiling}$ term in Eq. (12), while the shorter output reduces the N term. That’s why MSD can match LLMs in average acceptance length, but still shows a lower overall speedup ratio.

Acceptance Rate As shown in Figure 4, we compare the acceptance rate $n-\alpha$ of MSD and Baseline across different temperatures and positions n . MSD achieves a higher acceptance rate than Baseline across different n and temperature settings. As n increases under different temperature settings, both methods show a gradual decline in acceptance rate due to errors accumulation during inference. However, MSD consistently outperforms Baseline, demonstrating its robustness in generating accurate tokens of larger n .

5.3. Ablation study

In this section, we perform an ablation study to evaluate the contributions of MSD’s key components, including the input token decoupling strategy and the two-stage training strategy. Additionally, we ablate the input token decoupling strategy variants and the two-stage draft model training strategy variants. All experiments are performed on LLaVA-1.5-7B with a temperature of 0.

Ablation on Key Modules of MSD

As shown in Table 4, both the input tokens decoupling strategy and the two-stage training strategy contribute to MSD’s performance gains. Specifically, the decoupling strategy improves the average

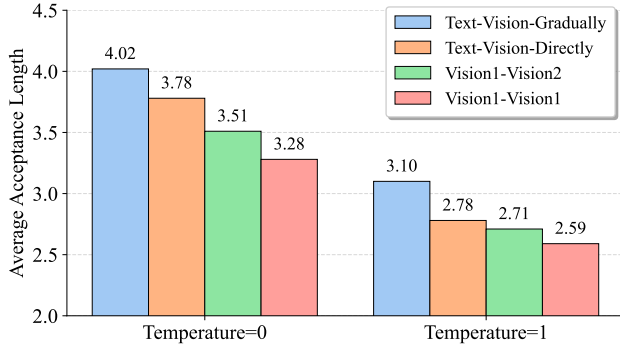


Figure 5. Impact of draft model training strategies, evaluated on a randomly sampled 100-example subset of ChartQA.

acceptance length by at least +0.37 across all tasks, while the two-stage training adds at least +0.65. The gain from the decoupling strategy highlights the importance of handling visual and textual tokens separately in the draft model, supporting the analysis in Sec. 4.1. MSD processes input tokens from different modalities in a way that aligns with their unique features. This boosts average acceptance length, especially on tasks that require fine-grained visual understanding, like ChartQA. The performance gain from the two-stage training strategy indicates that both language modeling ability and visual perception ability are important for the draft model, validating the analysis in Sec. 4.2. By combining both components, MSD achieves the highest average acceptance length across all tasks, outperforming the Baseline by 1.00 on average. This indicates that the two proposed improvements are complementary and can be used together to achieve a higher average acceptance length.

Ablation on Input Token Decoupling Strategy To validate the effectiveness of our input tokens decoupling strategy, we conduct an ablation study on different strategies for handling visual tokens. There are three different strategies for handling visual tokens: (1) Baseline: Visual tokens are concatenated with the next token’s hidden state, as introduced in Sec. 3.3. (2) Visual Feature: Visual tokens are represented by the hidden features produced by the LLM, without next-token concatenation. (3) Visual Embedding: Visual tokens are directly represented by their original embeddings from the input of the target model. As shown in Table 5, Baseline, which does not decouple visual tokens, performs worse than the other two methods, indicating the importance of decoupling visual and textual tokens in the draft model. Comparing the two decoupled methods, Visual Embedding achieves a slightly higher average acceptance length than Visual Feature. This suggests that using the original visual embeddings is better than using the hidden features from the LLM, as the original visual embed-

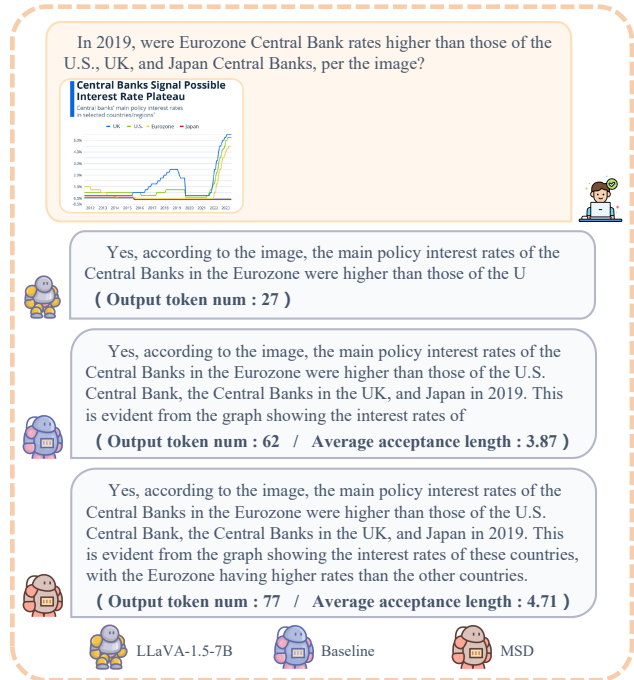


Figure 6. Chatbot responses using LLaVA-1.5-7B without speculation, with Baseline, and with MSD.

dings retain the clean visual information produced by the vision encoder, without being influenced by the language modeling process of the LLM.

Ablation on Two-Stage Training Strategy MSD uses a two-stage training strategy for draft model training, which first trains the draft model on a text-only instruction-tuning dataset and gradually transitions to a visual instruction-tuning dataset. We compare our two-stage training strategy (Text-Vision-Gradually) with the following training strategy variants: (1) Vision1-Vision1: The draft model is trained on the same visual instruction-tuning dataset (Vision1) in both stages. (2) Vision1-Vision2: The draft model is trained on two different visual instruction-tuning datasets (Vision1 and Vision2), one for each stage. (3) Text-Vision-Directly: The draft model is trained on a text-only instruction-tuning dataset in the first stage and then directly switches to a visual instruction-tuning dataset in the second stage. As shown in Figure 5, Text-Vision-Gradually achieves the highest average acceptance length. This indicates that the performance gain from the two-stage training strategy is not solely due to the increased amount of training data, but also due to language modeling ability acquisition through training on a text-only instruction-tuning dataset. A comparison between Text-Vision-Directly and Text-Vision-Gradually reveals that gradually transitioning from text-only to visual instruction-tuning data helps the

draft model to improve its visual perception ability while preserving its language modeling ability.

5.4. Multimodal Chatbot

To clearly show the performance of MSD, we visualize the chatbot responses generated by LLaVA-1.5-7B without speculative decoding, with the Baseline, and with MSD. As shown in Figure 6, for the same input and decoding time, MSD generates 77 tokens, while the Baseline and the model without MSD generate 62 and 27 tokens, respectively. MSD reduces decoding time and generates more tokens than both the Baseline and the model without speculative decoding, improving conversation efficiency.

5.5. Limitations and Future Works

MSD effectively reduces the average acceptance length gap between the speculative decoding of MLLMs and LLMs. Due to limited academic GPU resources, we only evaluate the effectiveness of MSD on LLaVA-1.5-7B and LLaVA-1.5-13B.

Future work could scale MSD to larger MLLMs with 34B parameters or more to further test its effectiveness. There is also a chance to extend MSD to more modalities, such as audio. Audio tokens have different characteristics compared to text or visual tokens. Future work should use a different processing strategy tailored to the characteristics of audio tokens in the draft model.

6. Conclusion

In this paper, we present Multimodal Speculative Decoding (MSD), a novel and effective approach to accelerating the inference of MLLMs without compromising accuracy. By analyzing the fundamental differences between LLMs and MLLMs, we identify two critical design principles for speculative decoding in the multimodal setting: (1) Text and visual tokens have fundamentally different characteristics and should be processed separately during drafting. (2) Both language modeling ability and visual perception capability are crucial for the draft model. Based on these principles, MSD first decouples input tokens of different modalities according to their characteristics in the draft model. Then, MSD adopts a two-stage training strategy for the draft model, enabling it to acquire both strong language modeling and visual understanding capabilities. Extensive experiments across diverse multimodal tasks confirm that MSD delivers a significant speedup ratio with no loss in accuracy.

Acknowledgements

This work was supported by the National Science Fund for Distinguished Young Scholars (No.62025603), the National Natural Science Foundation of China (No.

U21B2037, No. U22B2051, No. U23A20383, No. U21A20472, No. 62176222, No. 62176223, No. 62176226, No. 62072386, No. 62072387, No. 62072389, No. 62002305, and No. 62272401), and the Natural Science Foundation of Fujian Province of China (No. 2021J06003, No. 2022J06001).

References

- [1] Josh Achiam, Steven Adler, Sandhini Agarwal, Lama Ahmad, Ilge Akkaya, Florencia Leoni Aleman, Diogo Almeida, Janko Altenschmidt, Sam Altman, Shyamal Anadkat, et al. Gpt-4 technical report, 2023. 1
- [2] anon8231489123. Sharegpt. https://huggingface.co/datasets/anon8231489123/ShareGPT_Vicuna_unfiltered, 2023. Dataset available on Hugging Face. 2, 6
- [3] Jinze Bai, Shuai Bai, Shusheng Yang, Shijie Wang, Sinan Tan, Peng Wang, Junyang Lin, Chang Zhou, and Jingren Zhou. Qwen-vl: A versatile vision-language model for understanding, localization, text reading, and beyond, 2023. 3
- [4] Shuai Bai, Keqin Chen, Xuejing Liu, Jialin Wang, Wenbin Ge, Sibao Song, Kai Dang, Peng Wang, Shijie Wang, Jun Tang, Humen Zhong, Yuanzhi Zhu, Mingkun Yang, Zhaohai Li, Jianqiang Wan, Pengfei Wang, Wei Ding, Zheren Fu, Yiheng Xu, Jiabo Ye, Xi Zhang, Tianbao Xie, Zesen Cheng, Hang Zhang, Zhibo Yang, Haiyang Xu, and Junyang Lin. Qwen2.5-vl technical report, 2025. 1
- [5] Tianle Cai, Yuhong Li, Zhengyang Geng, Hongwu Peng, Jason D. Lee, Deming Chen, and Tri Dao. Medusa: Simple llm inference acceleration framework with multiple decoding heads, 2024. 2, 3
- [6] Jianjian Cao, Peng Ye, Shengze Li, Chong Yu, Yansong Tang, Jiwen Lu, and Tao Chen. Madtp: Multimodal alignment-guided dynamic token pruning for accelerating vision-language transformer. In *CVPR*, 2024. 3
- [7] Jian Chen, Vashisth Tiwari, Ranajoy Sadhukhan, Zhuoming Chen, Jinyuan Shi, Ian En-Hsu Yen, and Beidi Chen. Magicdec: Breaking the latency-throughput tradeoff for long context generation with speculative decoding. *arXiv preprint arXiv:2408.11049*, 2024. 7
- [8] Liang Chen, Haozhe Zhao, Tianyu Liu, Shuai Bai, Junyang Lin, Chang Zhou, and Baobao Chang. An image is worth 1/2 tokens after layer 2: Plug-and-play inference acceleration for large vision-language models. In *ECCV*, 2024. 3
- [9] Mengzhao Chen, Wenqi Shao, Peng Xu, Mingbao Lin, Kaipeng Zhang, Fei Chao, Rongrong Ji, Yu Qiao, and Ping Luo. Difftrate: Differentiable compression rate for efficient vision transformers. In *ICCV*, 2023. 1, 3
- [10] Mark Chen, Jerry Tworek, Heewoo Jun, Qiming Yuan, Henrique Ponde de Oliveira Pinto, Jared Kaplan, Harri Edwards, Yuri Burda, Nicholas Joseph, Greg Brockman, et al. Evaluating large language models trained on code. *arXiv preprint arXiv:2107.03374*, 2021. 8
- [11] Xinlei Chen, Hao Fang, Tsung-Yi Lin, Ramakrishna Vedantam, Saurabh Gupta, Piotr Dollár, and C Lawrence Zitnick. Microsoft coco captions: Data collection and evaluation server. *arXiv preprint arXiv:1504.00325*, 2015. 1

- [12] Zhe Chen, Jiannan Wu, Wenhai Wang, Weijie Su, Guo Chen, Sen Xing, Muyan Zhong, Qinglong Zhang, Xizhou Zhu, Lewei Lu, et al. Internvl: Scaling up vision foundation models and aligning for generic visual-linguistic tasks. In *CVPR*, 2024. 3
- [13] Karl Cobbe, Vineet Kosaraju, Mohammad Bavarian, Mark Chen, Heewoo Jun, Lukasz Kaiser, Matthias Plappert, Jerry Tworek, Jacob Hilton, Reiichiro Nakano, et al. Training verifiers to solve math word problems. *arXiv preprint arXiv:2110.14168*, 2021. 8
- [14] Tri Dao. Flashattention-2: Faster attention with better parallelism and work partitioning. In *ICLR*, 2023. 3
- [15] Tri Dao, Dan Fu, Stefano Ermon, Atri Rudra, and Christopher Ré. Flashattention: Fast and memory-efficient exact attention with io-awareness. In *NeurIPS*, 2022. 3
- [16] Chaoyou Fu, Peixian Chen, Yunhang Shen, Yulei Qin, Mengdan Zhang, Xu Lin, Jinrui Yang, Xiawu Zheng, Ke Li, Xing Sun, Yunsheng Wu, and Rongrong Ji. Mme: A comprehensive evaluation benchmark for multimodal large language models, 2023. 2, 6, 7
- [17] Yichao Fu, Peter Bailis, Ion Stoica, and Hao Zhang. Break the sequential dependency of llm inference using lookahead decoding. *arXiv preprint arXiv:2402.02057*, 2024. 2, 7
- [18] Mukul Gagrani, Raghav Goel, Wonseok Jeon, Junyoung Park, Mingu Lee, and Christopher Lott. On speculative decoding for multimodal large language models, 2024. 1, 2, 3, 7, 8
- [19] Yash Goyal, Tejas Khot, Douglas Summers-Stay, Dhruv Batra, and Devi Parikh. Making the v in vqa matter: Elevating the role of image understanding in visual question answering. In *CVPR*, pages 6904–6913, 2017. 1, 2, 6, 7, 8
- [20] Tianrui Guan, Fuxiao Liu, Xiyang Wu, Ruiqi Xian, Zongxia Li, Xiaoyu Liu, Xijun Wang, Lichang Chen, Furong Huang, Yaser Yacoob, et al. Hallusionbench: an advanced diagnostic suite for entangled language hallucination and visual illusion in large vision-language models. In *CVPR*, 2024. 1, 6, 7, 8
- [21] Aniruddha Kembhavi, Mike Salvato, Eric Kolve, Minjoon Seo, Hannaneh Hajishirzi, and Ali Farhadi. A diagram is worth a dozen images. In *ECCV*, pages 235–251, 2016. 2, 6, 7
- [22] Woosuk Kwon, Zhuohan Li, Siyuan Zhuang, Ying Sheng, Lianmin Zheng, Cody Hao Yu, Joseph Gonzalez, Hao Zhang, and Ion Stoica. Efficient memory management for large language model serving with pagedattention. In *SOSP*, 2023. 3
- [23] Yaniv Leviathan, Matan Kalman, and Yossi Matias. Fast inference from transformers via speculative decoding, 2023. 1, 3
- [24] Junnan Li, Dongxu Li, Silvio Savarese, and Steven Hoi. Blip-2: Bootstrapping language-image pre-training with frozen image encoders and large language models. In *ICML*, pages 19730–19742, 2023. 1
- [25] Shiyao Li, Yingchun Hu, Xuefei Ning, Xihui Liu, Ke Hong, Xiaotao Jia, Xiuhong Li, Yaqi Yan, Pei Ran, Guohao Dai, Shengen Yan, Huazhong Yang, and Yu Wang. Mbq: Modality-balanced quantization for large vision-language models, 2025. 1, 3
- [26] Wentong Li, Yuqian Yuan, Jian Liu, Dongqi Tang, Song Wang, Jie Qin, Jianke Zhu, and Lei Zhang. Tokenpacker: Efficient visual projector for multimodal llm, 2024. 3
- [27] Yuhui Li, Fangyun Wei, Chao Zhang, and Hongyang Zhang. EAGLE-2: Faster inference of language models with dynamic draft trees. In *EMNLP*, 2024. 2, 3
- [28] Yuhui Li, Fangyun Wei, Chao Zhang, and Hongyang Zhang. EAGLE: Speculative sampling requires rethinking feature uncertainty. In *ICML*, 2024. 2, 3, 4, 6, 7
- [29] Bin Lin, Zhenyu Tang, Yang Ye, Jiayi Cui, Bin Zhu, Peng Jin, Jinfa Huang, Junwu Zhang, Yatian Pang, Munan Ning, et al. Moe-llava: Mixture of experts for large vision-language models. *arXiv preprint arXiv:2401.15947*, 2024. 1, 3
- [30] Zhihang Lin, Mingbao Lin, Luxi Lin, and Rongrong Ji. Boosting multimodal large language models with visual tokens withdrawal for rapid inference. In *AAAI*, 2024. 3
- [31] Haotian Liu, Chunyuan Li, Yuheng Li, and Yong Jae Lee. Improved baselines with visual instruction tuning, 2023. 1, 3, 6, 8
- [32] Haotian Liu, Chunyuan Li, Yuheng Li, Bo Li, Yuanhan Zhang, Sheng Shen, and Yong Jae Lee. Llava-next: Improved reasoning, ocr, and world knowledge, January 2024. 1
- [33] Yuan Liu, Haodong Duan, Yuanhan Zhang, Bo Li, Songyang Zhang, Wangbo Zhao, Yike Yuan, Jiaqi Wang, Conghui He, Ziwei Liu, et al. Mmbench: Is your multi-modal model an all-around player?, 2023. 2, 6, 7
- [34] Pan Lu, Swaroop Mishra, Tanglin Xia, Liang Qiu, Kai-Wei Chang, Song-Chun Zhu, Oyvind Tafjord, Peter Clark, and Ashwin Kalyan. Learn to explain: Multimodal reasoning via thought chains for science question answering. In *NeurIPS*, pages 2507–2521, 2022. 7
- [35] Ahmed Masry, Do Long, Jia Qing Tan, and Enamul Joty, Shafiq An Hoque. ChartQA: A benchmark for question answering about charts with visual and logical reasoning. In *ACL*, 2022. 1, 2, 6, 7, 8
- [36] Brandon McKinzie et al. Mm1: Methods, analysis and insights from multimodal llm pre-training. In *ECCV*, 2024. 1, 3
- [37] Bryan A Plummer, Liwei Wang, Chris M Cervantes, Juan C Caicedo, Julia Hockenmaier, and Svetlana Lazebnik. Flickr30k entities: Collecting region-to-phrase correspondences for richer image-to-sentence models. In *ICCV*, 2015. 1
- [38] Alec Radford, Jong Wook Kim, Chris Hallacy, Aditya Ramesh, Gabriel Goh, Sandhini Agarwal, Girish Sastry, Amanda Askell, Pamela Mishkin, Jack Clark, Gretchen Krueger, and Ilya Sutskever. Learning transferable visual models from natural language supervision. In *ICML*, pages 8748–8763, 2021. 2
- [39] Dachuan Shi, Chaofan Tao, Anyi Rao, Zhendong Yang, Chun Yuan, and Jiaqi Wang. Crossget: cross-guided ensemble of tokens for accelerating vision-language transformers. In *ICML*, 2024. 3
- [40] Amanpreet Singh, Vivek Natarajan, Meet Shah, Yu Jiang, Xinlei Chen, Dhruv Batra, Devi Parikh, and Marcus

- Rohrbach. Towards vqa models that can read. In *CVPR*, 2019. 1, 2, 6, 7, 8
- [41] Gemini Team, Rohan Anil, Sebastian Borgeaud, Yonghui Wu, Jean-Baptiste Alayrac, Jiahui Yu, Radu Soricut, Johan Schalkwyk, Andrew M Dai, Anja Hauth, et al. Gemini: A family of highly capable multimodal models, 2023. 1
- [42] Changyuan Wang, Ziwei Wang, Xiuwei Xu, Yansong Tang, Jie Zhou, and Jiwen Lu. Q-vlm: Post-training quantization for large vision-language models. *arXiv preprint arXiv:2410.08119*, 2024. 1, 3
- [43] Maolin Wang, Yao Zhao, Jiajia Liu, Jingdong Chen, Chenyi Zhuang, Jinjie Gu, Ruocheng Guo, and Xiangyu Zhao. Large multimodal model compression via iterative efficient pruning and distillation. In *WWW*, 2024. 1, 3
- [44] Xinjian Wu, Fanhu Zeng, Xiudong Wang, Yunhe Wang, and Xinghao Chen. Ppt: Token pruning and pooling for efficient vision transformers, 2023. 1, 3
- [45] Qinghao Ye, Haiyang Xu, Guohai Xu, Jiabo Ye, Ming Yan, Yiyang Zhou, Junyang Wang, Anwen Hu, Pengcheng Shi, Yaya Shi, Chenliang Li, Yuanhong Xu, Hehong Chen, Junfeng Tian, Qi Qian, Ji Zhang, Fei Huang, and Jingren Zhou. mplug-owl: Modularization empowers large language models with multimodality, 2024. 3
- [46] Hanling Yi, Feng Lin, Hongbin Li, Ning Peiyang, Xiaotian Yu, and Rong Xiao. Generation meets verification: Accelerating large language model inference with smart parallel auto-correct decoding. In *ACL*, 2024. 3
- [47] Jun Zhang, Jue Wang, Huan Li, Lidan Shou, Ke Chen, Gang Chen, and Sharad Mehrotra. Draft& verify: Lossless large language model acceleration via self-speculative decoding. In *ACL*, 2024. 3
- [48] Lefan Zhang, Xiaodan Wang, Yanhua Huang, and Ruiwen Xu. Learning harmonized representations for speculative sampling, 2024. 3
- [49] Lianmin Zheng, Wei-Lin Chiang, Ying Sheng, Siyuan Zhuang, Zhanghao Wu, Yonghao Zhuang, Zi Lin, Zhuohan Li, Dacheng Li, Eric P. Xing, Hao Zhang, Joseph E. Gonzalez, and Ion Stoica. Judging llm-as-a-judge with mt-bench and chatbot arena. In *NeurIPS*, 2023. 8
- [50] Baichuan Zhou, Ying Hu, Xi Weng, Junlong Jia, Jie Luo, Xien Liu, Ji Wu, and Lei Huang. Tinyllava: A framework of small-scale large multimodal models. *arXiv preprint arXiv:2402.14289*, 2024. 3
- [51] Yichen Zhu, Minjie Zhu, Ning Liu, Zhiyuan Xu, and Yaxin Peng. Llava-phi: Efficient multi-modal assistant with small language model. In *EMCLR*, 2024. 3